

Enhancing the Performance of Butadiene Rubber and Natural Rubber Elastomers Using Green-Synthesized Carbon Quantum Dots Derived from Sugarcane Bagasse Waste

Arman Van , Mohamadamin Vosooghnia , Fereshteh Motiee*

Department of Chemistry, NT. C., Islamic Azad University, Tehran, Iran

* Corresponding authors: f_motiee@iau-tnb.ac.ir

Article History:

Received:
10 May 2025

Revised:
10 July 2025

Accepted:
29 September 2025

Published in Issue:
30 December 2025

© 2025 The Author(s). Published by the IOICC Press under the terms of the CC BY 4.0, Creative Commons Attribution License, which permits use, distribution and reproduction in any medium, provided the original work is properly cited.

Abstract

In this research work, carbon quantum dot nanoparticles derived from sugarcane bagasse were used in place of rubber industry aromatic oil and a portion of carbon black in five unique samples of the NR/BR elastomer mixture. The purpose of this research was to analyze the various mechanical, thermal, and rheological properties of the obtained mixtures. Comprehensive tests, including HR-TEM (High-Resolution Transmission Electron Microscopy), FESEM (Field Emission Scanning Electron Microscopy), DLS (Dynamic Light Scattering), and FTIR (Fourier Transform Infrared Spectroscopy), were employed to elucidate the properties of carbon quantum dots. In the following, elongation, tensile strength, abrasion resistance, rheometry, and Thermogravimetric analysis (TGA) tests were utilized to evaluate the mechanical, rheological, and thermal properties of the elastomeric mixtures. According to the collected results, among the synthesized samples, sample N₃ had the most outstanding thermal, rheological, and mechanical properties. Overall, it is predicted that the interaction of carbon quantum dots with NR/BR elastomer can lead to reduced environmental risks and increased mechanical properties in the rubber industry.

Keywords: Carbon Quantum Dots; Green Synthesis; Mechanical Properties; NR/BR Elastomers; Sugarcane Bagasse; Sustainable Materials; Thermal Stability

Cite this article: Van A, Vosooghnia M, Motiee F. Enhancing the Performance of Butadiene Rubber and Natural Rubber Elastomers Using Green-Synthesized Carbon Quantum Dots Derived from Sugarcane Bagasse Waste. *Int. J. Ind. Chem.* 2025; 16(4): 1-10. <https://doi.org/10.57647/j.ijic.2025.1604.16>

Graphical Abstract



Scheme 1. Illustration of the manufacturing process of NR/BR nanocomposites

1. Introduction

Elastomers, amorphous polymers with unique elastic properties, have garnered significant attention due to their viscoelastic behavior, high strain at break, and low Young's modulus [1]. Natural Rubber (NR), Butadiene Rubber (BR), and Styrene-Butadiene Rubber (SBR) are standard elastomers in the rubber industry. Blending these elastomers is an innovative approach to fabricating high-performance compounds [2,3]. For instance, natural rubber's distinctive properties, such as suitable elasticity, high oil resistance, aging resistance, and impermeability to air and ozone, make it a valuable component. However, polybutadiene, as a rubber, may not have all the physical properties required in a final product. Therefore, blending these two types of rubber is a novel and straightforward solution to enhance the synergy of elastomers [4,5,6]. Furthermore, fillers play a pivotal and undeniable role in improving the mechanical and rheological properties; without this group of materials, cross-linked elastomers would not exhibit significant properties. The most common reinforcing fillers are carbon black and silica, which can increase the tear resistance, tensile strength, and abrasion resistance of the elastomer. In fact, the amount of reinforcement provided by fillers is evaluated based on specific parameters, such as particle shape and size characteristics, volume fraction, particle morphology, and their dispersion state in the polymer matrix [7,8]. Despite the numerous positive properties that carbon black adds to elastomer compounds, these materials are produced through the incomplete combustion of petroleum products, which can contribute to increased environmental pollution. For this reason, researchers are currently seeking new fillers that have a lower environmental impact and retain the properties of carbon black [9,10]. Nanofillers, a novel generation of fillers, have the potential to significantly enhance the properties and performance of rubber products. Their high surface area-to-volume ratio facilitates stronger interactions with the elastomer, leading to improved properties. When present in tiny amounts in the polymer matrix, nanofillers with different morphologies form a large polymer-particle interfacial area due to their small dimensions. This initially causes proper processability and ultimately improves the desired properties, offering an optimistic outlook for the future of rubber products [11,12]. Carbon quantum dots (CQDs) are a fascinating group of carbon nanoparticles that have garnered significant attention in recent years due to their unique features. These include biocompatibility, high solubility, tunable functionalization, low toxicity, and luminescence properties. With diameters ranging from 3 to 20 nm and a quasi-spherical shape with amorphous to nanocrystalline cores, these nanoparticles are a versatile tool. Their unique

properties make them suitable for a wide range of applications, including chemical and biological sensors, drug delivery systems, photocatalysts, and bioimaging. The use of natural precursors (sugarcane bagasse) further enhances their appeal, offering an innovative way to synthesize carbon quantum dots and reduce the toxicity of the system in terms of chemistry [13,14,15]. This research aimed to replace the aromatic oil used in the rubber industry and part of the carbon black in NR/BR elastomeric mixtures with liquid-phase-synthesized carbon quantum dots derived from sugarcane bagasse. This innovative approach represents a significant step toward mitigating the adverse environmental impacts of elastomer production. The research also investigated the effect and role of carbon quantum dot samples in improving the mechanical, rheological, and thermal properties of the developed mixtures.

2. Materials and methods

2.1. Materials

The materials utilized in this study were selected based on their compatibility with the experimental requirements and objectives. Toluene ($\geq 99.5\%$), generated by (Merck, Germany) was used as the solvent in the CQD synthesis process. Sugarcane Bagasse purchased from (Ahvaz, Iran) was used to develop carbon quantum dot samples. BR 1500 (1502), sourced from (Arak Petrochemical Company, Iran), and SMR 20 (NR), obtained from (THE AHAU (GM) Company, Malaysia), were used as the raw elastomers. In addition, Mixing agents include Carbon Black (N-330) fabricated by (Pars et al. Company, Iran), Aromatic oil 250 made by (Iranol company, Iran), Stearic Acid made by (klk company, Malaysia), Zinc Oxide (ZnO) made by (Shokohieh company, Iran), Anti-ozone (4020) IPPD made by (Stair Chemical, China), TMQ accelerator made by (HENAN company, China), Ordinary sulfur for Vulcanization made by (Iran's Tesdak Company, Iran), CZ accelerator made by (MOI Company, China), and paraffin wax made by (Iran Shimi Company, Iran) were purchased.

2.1. Methods

2.2.1. Synthesising of Carbon Quantum Dot (CQD)

Sugarcane bagasse was selected as the precursor material due to its accessibility, low cost, and ecological benefits. Carbon quantum dots were produced by modifying the method described by Thambiraj et al. in 2016 [16]. We placed a predetermined amount of dry sugarcane bagasse inside the electric furnace and set its temperature to 300 °C for 30 minutes.

Table 1. Formulation of manufactured NR/BR Nanocomposites

Component (phr)	Blank sample	N ₁	N ₂	N ₃	N ₄	N ₅
1 SMR 20 (NR)	80	80	80	80	80	80
2 BR 1500 (1502)	20	20	20	20	20	20
3 Carbon Black (N-330)	50	50	45	45	40	40
4 Aromatic Oil	5	5	5	5	5	5
5 St. Acid	2	2	2	2	2	2
6 ZnO	4	4	4	4	4	4
7 IPPD (4020)	1.5	1.5	1.5	1.5	1.5	1.5
8 TMQ	2	2	2	2	2	2
9 S	1.5	1.5	1.5	1.5	1.5	1.5
10 CZ	1	1	1	1	1	1
11 Paraffin Wax	2	2	2	0	2	0
12 phr total mass balance	169	169	164	162	159	157

Then, we weighed 1 gram of semi-carbonized bagasse and added 100 mL of toluene to it. Then, the resulting mixture is placed on the heater stirrer for 24 hours until it becomes a single phase. Then, we placed the material obtained from the ultrasonic device in the centrifuge and spun it for 45 minutes at 9000 revolutions. Finally, we collected the supernatant from the centrifuge for further tests and characterization.

2.2.2. Production of NR/BR Nanocomposites

Six exclusive formulations, including the blank sample and five new samples, were manufactured at room temperature with a relative humidity of 45%. In this study, the amount of carbon black and the presence or absence of paraffin wax were considered as variable parameters or differences between the samples.

As is clear from Table 1, the amount of carbon black consumed in different samples varies. Furthermore, in the blank sample formulation, a standard aromatic oil commonly used in the rubber industry was employed. In contrast, the formulation of the five newly developed samples utilized a carbon quantum dot solution as a substitute for the standard aromatic oil typically used in the rubber industry.

In other words, the amount of aromatic oil in Table 1 in samples N₁ to N₅ indicates the amount of carbon quantum dot consumed. The samples were made by a double roller mill in four consecutive steps. In the first step, the mastication or softening process of the elastomeric compound was carried out for 15 minutes. In the second step, the filler was added to the elastomeric compound and mixed for 10 minutes.

Then, the powdered materials were added for about 5 minutes. Finally, curing agents were added to the elastomeric compound, a process that also took 5 minutes. After mixing, the compounds were allowed to rest for 24 hours at controlled temperature and humidity. Then, the

rheological, mechanical, and thermal properties of the mixtures were evaluated.

2.3. Characterization studies

This section is classified into two different parts. The first part involves characterizing tests related to the control of carbon quantum dots' properties, and the second part consists of characterizing tests associated with the control of rheological, mechanical, and thermal properties of rubber samples developed with carbon quantum dots.

2.3.1. Characterization of carbon quantum dots

Various optical and spectroscopic techniques characterized the prepared carbon quantum dots.

2.3.1.1. FT-IR (Fourier Transform Infrared Spectroscopy)

This test was used to study the surface functional groups of carbon quantum dots. The changes were recorded by Bruker Tensor II spectroscopy, which has a spectral range of 650 to 4000 cm⁻¹ at room temperature.

2.3.1.2. DLS (Dynamic Light Scattering)

This test is used to study nanoparticles and investigate their particle size in liquids. This method focuses on the rate of change in the intensity of visible light scattered by particles as they move randomly due to Brownian motion in a liquid medium. A 10 cm³ sample of carbon quantum dots was consumed to evaluate and measure nanoparticles using a Scatteroscope-Quidix instrument.

2.3.1.3. HR-TEM (High-resolution Transmission Electron Microscope)

The particle size, dispersion, and morphology of the carbon quantum dots sample were evaluated using an FEI-Tecna F20 instrument. For sampling, a few drops of CQD solution were placed on a carbon-coated grid. The sample was then prepared for imaging after the carbon quantum dot solution had dried entirely on the grid. Moreover, a histogram of the average particle size was obtained using the same instrument.

2.3.1.4. FESEM (Field Emission Scanning Electron Microscope)

This test was performed using a Zeiss-EIGMA300 instrument to examine the morphology and surface images of carbon quantum dot samples. The primary advantage of FESEM analysis over conventional SEM analysis is its significantly improved resolution, which is

attributed to the use of a field-emission electron source. For sampling, a portion of the CQD sample, which was dried by freeze-drying, was inserted into the gold coating and analyzed. The sample components, in terms of percentage, were also analyzed using the EDS (energy-dispersive X-ray spectroscopy) detector of this instrument at an accelerating voltage of 25 kV.

2.3.2. Characterization of NR/BR Nanocomposites

Various mechanical, rheological, and thermal tests were conducted to evaluate the manufactured NR/BR nanocomposites.

2.3.2.1. Tensile strength test

This test, performed using a tensile instrument (Universal-M350-5KN model) at a speed of 500 mm/min in accordance with ASTM D412, is considered one of the most prominent mechanical tests for rubbers. To prepare tensile test samples, dumbbell-shaped patterns must be cut from a flat rubber sheet with a thickness of approximately 2 mm.

These dumbbell-shaped samples are then subjected to tension in a tensile testing machine, and the force required to stretch them to the point of breaking is recorded. By dividing the force by the initial cross-sectional area of the dumbbell, the amount of tensile strength at multiple levels is calculated and recorded.

The amount of sample expansion is calculated by dividing the increase in length by the initial length, expressed as a percentage of the initial length. The amount of stretch before the sample breaks represents its modulus of elasticity.

Modulus is the amount of stretch (stress) at a specific elongation, usually at 100%, 200%, and 300%. Another well-known application of the tensile test is to determine the dispersion level of materials in a rubber compound during the mixing stage.

2.3.2.2. Abrasion test

Abrasion refers to the gradual loss of the rubber surface in contact with an uneven surface, which is the basis of all abrasion tests. The measurement of the percentage weight loss after the test, per cubic millimeter, is the conventional method for determining abrasion.

The amount of abrasion is calculated by dividing the difference between the secondary weight (after the wear test) and the primary weight (before the wear test) by the initial weight. This test was performed according to ISO 4649 (10 N load, 0.3 m/s, SiC abrasive, 40 m sliding distance) using the AB602103 Abrasion Testing Machine from Bareiss Company in Germany.

2.3.2.3. Rheometry test

The device (MDR-HIWA 900), which features a conical disk and oscillating motion rather than rotary motion, was used to conduct this test, aiming to study and determine the curing state. This test, which follows the ASTM D 5289 standard, measures main rheological parameters, including maximum torque (M_H), minimum torque (M_L), optimum curing time (T_{S2}), intermediate curing time (T_{C50}), curing time (T_{C90}), and curing rate index (CRI).

2.3.2.4. TGA (Thermogravimetric Analysis)

This test was used to study the thermal behavior of the fabricated nanocomposite. This analysis displays a diagram where the x-axis represents the desired temperature range and the y-axis represents the mass loss of the material. In fact, this experiment begins at a specific and arbitrary temperature and increases at a constant rate, ultimately reaching the final temperature determined. Additionally, this analysis was conducted using a TGA Q600 instrument manufactured by TA Instruments in the United States. This test was performed in the temperature range of 25 to 800 °C and at a temperature rate of 10 °C/min. This test was performed in the temperature range of 25 to 400 °C in an argon atmosphere and from 400 to 800 °C in an air atmosphere.

2.3.2.5. FESEM (Field Emission Scanning Electron Microscope)

FESEM was used to assess the filler-elastomer interaction and the degree of dispersion of components in the elastomeric mixture.

3. Results and discussion

3.1. Carbon quantum dot characterization

3.1.2. HR-TEM (High-resolution Transmission Electron Microscope)

Fig. 1a and 1b are HR-TEM images of the carbon quantum dot sample. As can be seen, these nanoparticles have a nearly spherical morphology and uniform dispersion. In addition, it is worth noting that they have a structure similar to that of graphite sheets [17].

Fig. 1c also shows the average particle size of 1.27 nm among 556 particles, which indicates the small size of the particles compared to previous studies [18].

3.1.2. FESEM (Field Emission Scanning Electron Microscope)

Figs. 1d and 1e are FESEM images of the carbon quantum dot sample.

Based on the analysis data, these nanoparticles have a rough surface and quasi-spherical morphology. Fig. 1f shows the EDS map, which suggests that the synthesized

carbon quantum dot sample contains approximately 80% carbon and 20% oxygen [19].

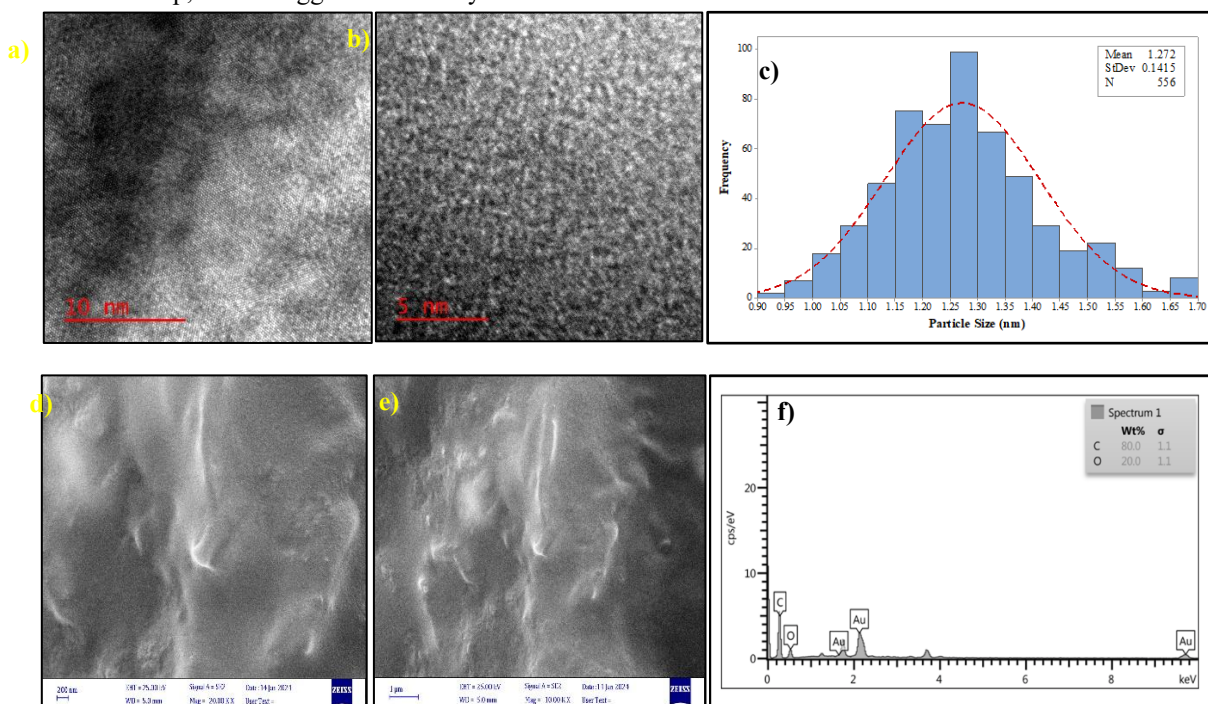


Figure 1. HR-TEM images of the CQD sample. a) Scale of 10 nm, b) Scale of 5 nm, c) Particle size histogram of the carbon quantum dot sample with an average of 1.272 ± 0.14 nm among 556 particles corresponding to image (b), FESEM Images of CQD sample. d) At $1\mu\text{m}$ scale, e) At 200 nm scale, f) EDS diagram representing 80% pure carbon and 20% oxygen

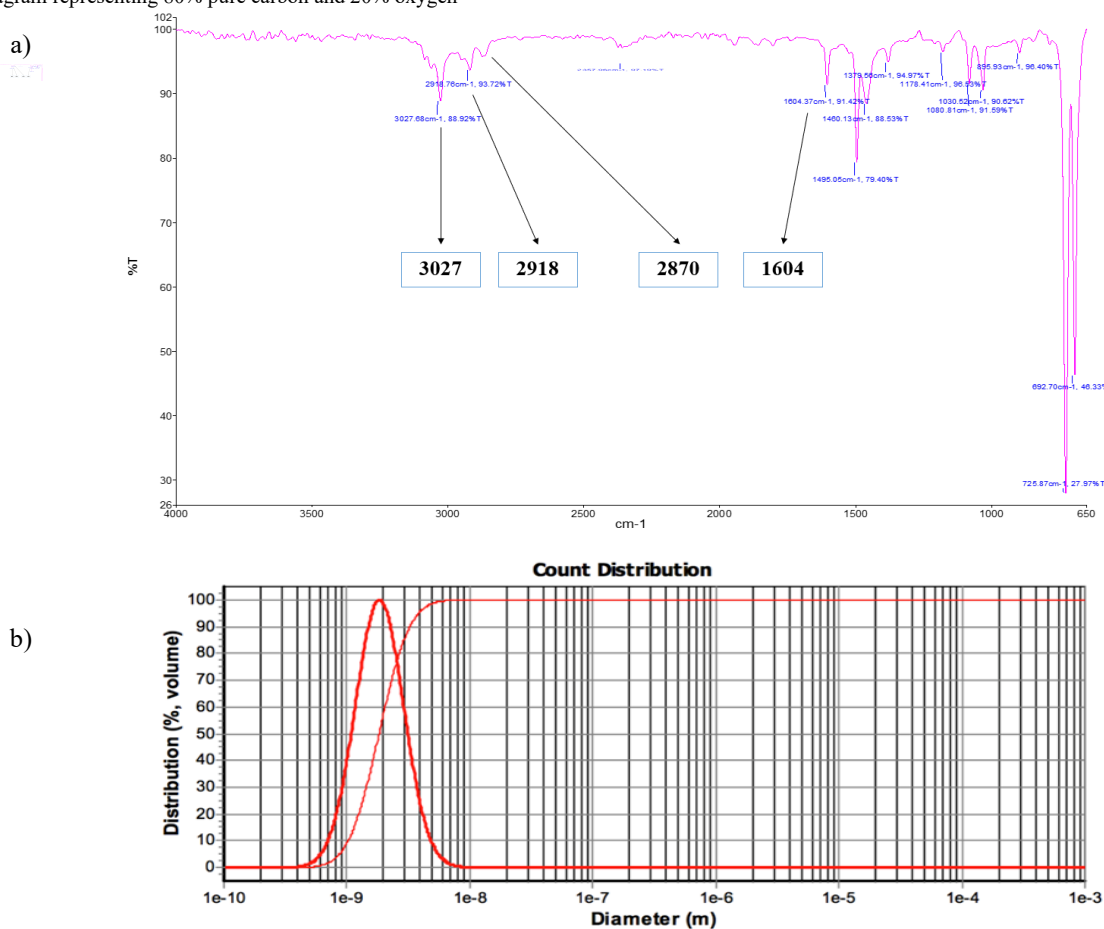


Figure 2. a) FT-IR spectrum of developed CQD sample, b) DLS analysis of CQD sample, with an average size of 1.84 nm

3.1.3. FT-IR (Fourier Transform Infrared) Spectroscopy

Fig. 2a shows the FT-IR spectrum, which was used to identify the functional groups. The first prominent peak was found at (1604 cm^{-1}), which is related to the aromatic C=C. Two strong absorption bands are also observed at (2919 cm^{-1}) and (2871 cm^{-1}), which are explained by the C=C stretching vibration of the methyl or methylene groups in the CQD with toluene. In addition, a weak absorption peak at (3085 cm^{-1}) can be confirmed by the presence of hydrogen bonds, indicating the presence of O-H functional groups on the surface of the carbon quantum dots [16,20,15].

3.1.4. DLS (Dynamic Light Scattering)

Fig. 2b displays a DLS test performed to confirm the HR-TEM results on particle size. This diagram illustrates the particle size distribution of the sample based on the percentage of particles in the sample. From this diagram, it can be seen that the average particle size, as determined by the peak obtained, is 1.84 nm, which is in suitable agreement with the HR-TEM results [21,22].

3.2. Mechanical and thermal attributes of NR/BR Nanocomposites

3.2.1. Elongation

As can be inferred from Table 2, all the composites made with carbon quantum dots have higher elongation at break than the industrial blank sample, and sample N₃ has the highest elongation at break. The primary reason for incorporating nanofillers into the polymer matrix system is to enhance the mechanical properties of polymer nanocomposites. In other words, adding nanofillers to an elastomer-elastomer blend system acts as a reinforcing agent [12]. Based on the results of previous research, the proper interaction between two or more types of fillers also enhances the dispersion of the filler and the effective transfer of stress from the matrix, leading to improvements in the mechanical and dynamic properties of the composite. These hybrid nanocomposites generally exhibit an increase in elongation at break compared to single-filler microcomposites [23].

3.2.2. Abrasion

Based on the data in Table 2, the abrasion resistance of samples N₁ to N₅ is lower than that of the blank sample, indicating a decrease in abrasion loss in these five samples. In previous research, the abrasion properties of rubber have been improved by adding graphite-like fillers, which can be attributed to the remarkable impact of the

size and shape of the filler particles on the tribological properties of polymers [24].

Moreover, increasing the crosslink density improves the abrasion resistance, which is the result of the formation of stronger chemical bonds between polymer chains within the nanocomposites. In fact, the appropriate arrangement and structure of crosslinks provide better integrity for the nanocomposite and increase its abrasion resistance [25].

3.2.3. Tensile strength

In terms of tensile strength, which indicates the level of stress tolerance, the synthesized samples with carbon quantum dots are also slightly higher than the blank sample, with the highest value observed in samples N₂ and N₃. Carbon nanocomposites possess high modulus, tensile strength, and a large surface-to-volume ratio.

When added to the elastomer mixture, they interact with rubber particles, thereby limiting the breakage of rubber molecular chains and significantly enhancing the mechanical properties of the rubber composites [26]. However, in this test, based on different carbon quantum dot loadings, the tensile strength increased to a maximum value, then decreased with higher loadings.

This can be justified by the improper dispersion of nanofiller at higher filler loadings, which leads to the formation of numerous stress-causing areas and weak interactions [12].

3.2.4. Modulus at 100% and 300% points

The modulus or stress-strain ratio at 100% elongation in the samples containing carbon quantum dots is completely improved compared to the blank sample. In comparison, at 300% elongation, only the N₃ sample has a higher modulus than the blank sample. Generally, the presence of carbon nanofillers, which are harder than the soft rubber matrix, improves the cross-linking density of the rubber chains and consequently increases the elastic modulus of the polymer matrix [27].

Furthermore, according to previous research, the Young's modulus depends on the particle size and the balance of dispersion of the nanofiller layers in the elastomeric mixture. The smaller the particle size and the more efficient the dispersion of the nanofillers, the higher the modulus [28]. ANOVA verified significant differences ($p < 0.05$) between formulations in all mechanical data.

3.2.5. TGA of N₃ mixture

Fig. 3d shows the TGA and DTG diagrams of sample N₃. According to the results of the differential thermogravimetric (DTG) diagram, this sample was

degraded at 3 points. The first thermal degradation point occurred at 363 °C, followed by a second point at 406 °C, and the last degradation point was at 519 °C. Additionally, the tested sample exhibited a 78% weight change. Previous studies have proven that the thermal stability of polymer nanocomposites is improved by the presence of

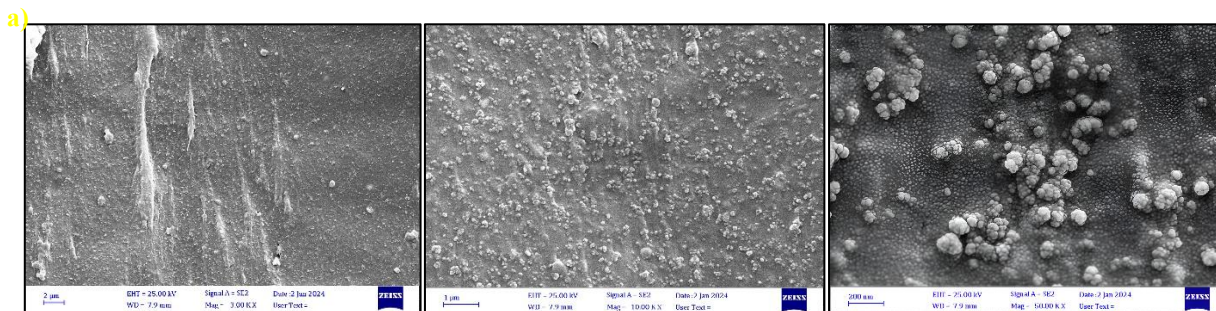
nanofillers in the rubber matrix. The primary reason for the enhancement in the thermal properties of nanocomposites is the formation of irregular paths by nanofillers, which hinder direct heat transfer to the degrading polymer composition and shield the underlying elastomer from thermal degradation.

Table 2. Mechanical result of manufactured NR/BR Nanocomposites (P-value < 0.05)

Sample	Stress (MPa)	Elongation (%)	Modulus (100%)	Modulus (300%)	Abrasion (mm ³)
N ₁	24.33 ± 0.84	400 ± 7.40	3.25 ± 0.21	5.70 ± 0.06	120.5 ± 0.63
N ₂	26.84 ± 0.86	411 ± 4.98	2.82 ± 0.19	5.40 ± 0.17	118.8 ± 2.55
N ₃	26.84 ± 0.76	414 ± 8.80	3.32 ± 0.25	6.10 ± 0.05	118.8 ± 1.88
N ₄	25.45 ± 0.6	414 ± 4.54	2.42 ± 0.20	4.75 ± 0.15	117.9 ± 1.34
N ₅	25.95 ± 0.89	402 ± 5.55	2.76 ± 0.22	5.32 ± 0.13	120.4 ± 1.52
Blank Sample	24.15 ± 0.81	392 ± 4.64	2.34 ± 0.20	5.75 ± 0.06	129.9 ± 2.22

Table 3. Rheological result of manufactured NR/BR Nanocomposites

Sample	M _H (dN/m)	M _L (dN/m)	M _H – M _L ΔH	CRI Min ⁻¹	T _{S2} (Sec)	T _{C90} (Sec)
N ₁	8.96	1.62	7.34	60.11	108	194
N ₂	8.53	1.62	6.90	64.62	113	205
N ₃	8.86	1.83	7.02	67.66	110	186
N ₄	8.00	1.51	6.49	61.94	116	198
N ₅	8.10	1.51	6.59	69.48	110	190
Blank Sample	7.93	1.22	6.71	52.06	134	238



d)

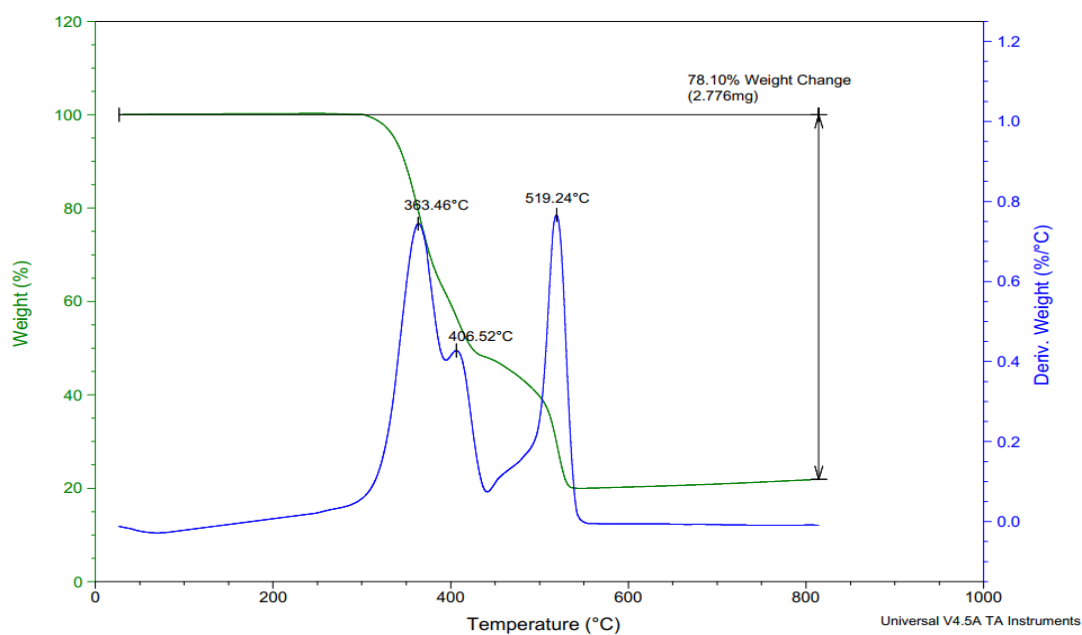


Figure 3. FESEM Images of N₃ sample. a) At 2 μm nm scale, b) At 1 μm, c) At 200 nm. d) TGA analysis of N₃ sample

Table 4. Key parameters of TGA analysis of N₃ mixture

Sample	T _{5%} (°C)	T _{max} (°C)	Char Yield (%)
N ₃	336.6	545	21.9

Also, the proper dispersion of nanofillers in the polymer matrix prevents premature thermal degradation of the elastomer.

Consequently, the presence of nanofillers actually maintains the thermal stability of the samples and increases the initial thermal degradation temperature of the composites [29,30].

3.2.6. FESEM of N₃ mixture

Figs. 3a, 3b, and 3c illustrate FESEM images of carbon quantum dot nanoparticles at multiple scales. This test was performed to study the morphology, distribution, dispersion, and extent of filler-elastomer interaction of nanoparticles in the most prominent developed rubber compound (N₃) [31].

By overloading nanoparticles in the polymer matrix, the distance between the particles decreases, which can lead to the formation of agglomerates. More precisely, the stronger than usual van der Waals attraction created between these nanofillers increases the tendency to aggregate in the polymer matrix [32]. However, as is obvious from the FESEM images, this sample has a uniform dispersion and distribution, indicating a balanced and efficient formulation.

3.3. Rheological attributes of NR/BR Nanocomposites

3.3.1. Optimum curing time (T_{S2}) and curing time in 90% mode (T_{C90})

As shown in Table 3, the optimum curing time (T_{S2}) and curing time at 90% strength (T_{C90}) have decreased compared to the industrial blank sample. The time when the torque is two units greater than the minimum is referred to as the optimum curing or scorching time (T_{S2}), and the time it takes for 90% of the cross-links in the rubber compounds to form is called the curing time (T_{C90}). These two parameters have an inverse relationship with the curing rate index. Generally, the presence of nanoparticles with suitable dispersion reduces the optimum curing time and curing time [33]. Also, polar agents on the surface of nanoparticles can accelerate the formation of filler-elastomer interactions during the curing process, thereby reducing (T_{S2}) and (T_{C90}) [34].

3.3.2. The amount of torque at the minimum and maximum points (M_L, M_H)

According to the data in Table 3, the maximum torque (M_H) in samples (N₁-N₅) and the difference between the

maximum torque and the minimum torque in samples (N₁-N₃) are higher than those of the commercial blank sample. This parameter is indirectly related to the density of crosslinks formed during the curing process. The higher this value, the higher the density of crosslinks, which affects the final properties of the polymer matrix, such as hardness and modulus [27]. Also, the efficient interaction of polymer chains with nanoparticles (CQDs) may be the reason for the improvement in maximum torque, which increases the stiffness of the elastomeric mixture [34].

3.3.3. Curing Rate Index (CRI)

As mentioned, if the optimal curing time and curing time are reduced, the curing rate index increases. The reason for this increase can be attributed to the carbonaceous nature of the carbon quantum dot nanoparticles, which facilitates improved heat transfer within the elastomeric matrix during the vulcanization process. The overall changes in the curing features in the samples containing CQD are also due to the larger specific surface area and more interaction with the polymer chains. As expected, the curing speed in the samples consisting of carbon quantum dots is higher than the blank sample, and sample N₃ has the highest curing rate index [34].

4. Conclusion

Overall, the developed NR/BR nanocomposites containing carbon quantum dots as a substitute for aromatic oil and part of carbon black did not display any decrease in rheological, mechanical, and thermal properties compared to the industrial blank sample, which is due to the compatibility of these nanoparticles with the polymer matrix and the balance in the formulation. In addition to proper interaction with the rubber matrix, the synthesized carbon quantum dots formed an appropriate dispersion in the rubber mixture, which can be attributed to their small size, carbon-based nature, and large specific surface area. A key finding in this study was the amount of carbon quantum dot nanoparticles added to enhance mechanical and rheological properties. Sample N₃ had the highest elongation, Young's modulus, tensile strength, and the lowest abrasion rate in comparison to other manufactured samples. Ultimately, in terms of environmental considerations, synthesized carbon quantum dots can be a suitable alternative to aromatic oils in the rubber industry due to their acceptable toxicity, suitable solubility, and low heat loss.

Acknowledgements

We would like to sincerely thank the Abundant contributions and valuable services of the experts at the

Iran Rubber Industry Research Center in conducting this research.

Authors Contribution

All the authors have participated sufficiently in the intellectual content, conception and design of this work or the analysis and interpretation of the data (when applicable), as well as the writing of the manuscript.

Data availability

All data generated or analyzed during this study are included in this published article.

Conflict of interests

The author states that there is no conflict of interest.

References

- [1] Joshi AM. Rubbers and Elastomers in Specialty Applications. In: Specialty Polymers and Materials. Apple Academic Press; 2025:293-314.
- [2] Fazli A, Rodrigue D. Waste rubber recycling: A review on the evolution and properties of thermoplastic elastomers. *Materials (Basel)*. 2020;13(3):782.
- [3] Kamankesh P, Ghayedi Z. *Archive of SID*. ir *Archive of SID*. ir *Archive of SID*. ir *Archive of SID*. ir. *J Sci Eng Elit*. 2023;12(47):84-92.
- [4] Bokobza L. Natural rubber nanocomposites: A review. *Nanomaterials*. 2019;9(1). <https://doi.org/10.3390/nano9010012>
- [5] Jovanović S, Samaržija-Jovanović S, Marković G, Jovanović V, Adamović T, Marinović-Cincović M. Ternary NR/BR/SBR rubber blend nanocomposites. *J Thermoplast Compos Mater*. 2018;31(2):265-287. <https://doi.org/10.1177/0892705717697778>
- [6] Alipour A. Study the morphology, microstructure. In: International Conference on Nanotechnology and Biosensors IPCBEE. Vol 25. 2011:44-48.
- [7] Bokobza L. Elastomer Nanocomposites : Effect of Filler – Matrix and Filler – Filler Interactions. Published online 2023.
- [8] Srivastava SK, Mishra YK. Nanocarbon reinforced rubber nanocomposites: Detailed insights about mechanical, dynamical mechanical properties, payne, and mullin effects. *Nanomaterials*. 2018;8(11):1-56. <https://doi.org/10.3390/nano8110945>
- [9] Fan Y, Fowler GD, Zhao M. The Past, Present and Future of Carbon Black as a Rubber Reinforcing Filler – A Review. Vol 247. Elsevier B.V.; 2020. <https://doi.org/10.1016/j.jclepro.2019.119115>
- [10] Dwivedi C, Manjare S, Rajan SK. Recycling of waste tire by pyrolysis to recover carbon black: Alternative & environment-friendly reinforcing filler for natural rubber compounds. *Compos Part B Eng*. 2020;200(July):108346. <https://doi.org/10.1016/j.compositesb.2020.108346>
- [11] Casalini R, Bogoslovov R, Qadri SB, Roland CM. Nanofiller reinforcement of elastomeric polyurea. *Polymer (Guildf)*. 2012;53(6):1282-1287. <https://doi.org/10.1016/j.polymer.2012.01.034>
- [12] Abd Razak J, Haji Ahmad S, Mohamad N, et al. Role of Nanofillers in Elastomer–Elastomer Blends. *INC*; 2024. <https://doi.org/10.1016/B978-0-323-88655-0.00006-9>
- [13] Zhao DL, Chung TS. Applications of carbon quantum dots (CQDs) in membrane technologies: A review. *Water Res*. 2018;147:43-49. <https://doi.org/10.1016/j.watres.2018.09.040>
- [14] Das R, Bandyopadhyay R, Pramanik P. Carbon quantum dots from natural resource: A review. *Mater Today Chem*. 2018;8:96-109. <https://doi.org/10.1016/j.mtchem.2018.03.003>
- [15] Arumugham T, Alagumuthu M, Amimodu RG, Munusamy S, Iyer SK. A sustainable synthesis of green carbon quantum dot (CQD) from *Catharanthus roseus* (white flowering plant) leaves and investigation of its dual fluorescence responsive behavior in multi-ion detection and biological applications. *Sustain Mater Technol*. 2020;23:e00138. <https://doi.org/10.1016/j.susmat.2019.e00138>
- [16] S. T, D. RS. Green synthesis of highly fluorescent carbon quantum dots from sugarcane bagasse pulp. *Appl Surf Sci*. 2016;390:435-443. <https://doi.org/10.1016/j.apsusc.2016.08.106>
- [17] Zhou Z, Li Z, Wang J, Wu Z, Fu Y. Solvothermal synthesis of nitrogen-doped carbon quantum dots for the sensitive detection of azithromycin. *Nanotechnology*. 2023;34(4). <https://doi.org/10.1088/1361-6528/ac9d44>
- [18] Ateia EE, Rabie O, Mohamed AT. Assessment of the correlation between optical properties and CQD preparation approaches. *Eur Phys J Plus*. 2024;139(1). <https://doi.org/10.1140/epjp/s13360-023-04811-7>
- [19] Nizam NUM, Hanafiah MM, Mahmoudi E, Mohammad AW. Synthesis of highly fluorescent carbon quantum dots from rubber seed shells for the adsorption and photocatalytic degradation of dyes. *Sci Rep*. 2023;13(1):1-17. <https://doi.org/10.1038/s41598-023-40069-w>
- [20] Aslan M, Eskalen H, Kavgaci M. Carbon Quantum Dot (CQD) Nanoparticles Synthesized by Sucrose and Urea: Application as Reinforcement Effect on Al–Mg–Cu–Zn Composite. *Russ J Gen Chem*. 2023;93(8):2152-2160. <https://doi.org/10.1134/S1070363223080236>
- [21] Marouzi S, Darroudi M, Hekmat A, Sadri K, Kazemi Oskuee R. One-pot hydrothermal synthesis of carbon quantum dots from *Salvia hispanica L.* seeds and investigation of their biodistribution, and cytotoxicity effects. *J Environ Chem Eng*. 2021;9(4):105461. <https://doi.org/10.1016/j.jece.2021.105461>
- [22] Huang S, Li W, Han P, et al. Carbon quantum dots: Synthesis, properties, and sensing applications as a potential clinical analytical method. *Anal Methods*. 2019;11(17):2240-2258. <https://doi.org/10.1039/c9ay00068b>
- [23] Thongchom C, Refahati N, Saffari PR, et al. An experimental study on the effect of nanomaterials and fibers on the mechanical properties of polymer composites. *Buildings*. 2022;12(1). <https://doi.org/10.3390/buildings12010007>
- [24] Ismail MN, Khalaf AI. Styrene–butadiene rubber/graphite powder composites: Rheometrical, physicochemical, and morphological properties. *J Appl Polym Sci*. 2011;120(1):298-304.
- [25] Srinivas J. The Synergistic effect of nanoclay / nanosilica on mechanical properties and swelling resistance of ternary rubber (

- NR / SBR / NBR) blends nanocomposites. Published online 2023:1-31.
- [26] Zhang J, Gu Z, Meng C, Wang J, Sui J. Morphology and selected properties of NR/BR/CNT nanocomposites effect of ethanol-assisted mixing. *Polimery*. 2023;68(5):251-258.
- [27] Tang LC, Zhao L, Qiang F, Wu Q, Gong LX, Peng JP. Mechanical properties of rubber nanocomposites containing carbon nanofillers. In: *Carbon-Based Nanofillers and Their Rubber Nanocomposites*. Elsevier; 2019:367-423.
- [28] Azizli MJ, Mokhtary M, Khonakdar HA, Goodarzi V. Hybrid Rubber Nanocomposites Based on XNBR/EPDM: Select the Best Dispersion Type from Different Nanofillers in the Presence of a Compatibilizer. *J Inorg Organomet Polym Mater*. 2020;30(7):2533-2550.
<https://doi.org/10.1007/s10904-020-01502-z>
- [29] Srivastava SK. Thermal properties of rubber nanocomposites based on carbon nanofillers. In: *Carbon-Based Nanofillers and Their Rubber Nanocomposites*. Elsevier; 2019:287-324.
- [30] Saha T, Bhowmick AK. Influence of nanofiller on thermal degradation resistance of hydrogenated nitrile butadiene rubber. *Rubber Chem Technol*. 2019;92(2):263-285.
- [31] Srinivas J, Jagatheeshwaran MS, Elayaperumal A, Vishvanathperumal S. The effect of nanoclay on mechanical and swelling resistance properties of ternary rubber (NR/SBR/NBR) blends nanocomposites. Published online 2023.
- [32] Namitha LK, Chameswary J, Ananthakumar S, Sebastian MT. Effect of micro-and nano-fillers on the properties of silicone rubber-alumina flexible microwave substrate. *Ceram Int*. 2013;39(6):7077-7087.
- [33] Damircheli M, MajidiRad A. The influence of the dispersion method on the morphological, curing, and mechanical properties of NR/SBR reinforced with nano-calcium carbonate. *Polymers (Basel)*. 2023;15(13):2963.
- [34] Barghamadi M, Karrabi M, Ghoreishy MHR, Mohammadian-Gezaz S. Effects of two types of nanoparticles on the cure, rheological, and mechanical properties of rubber nanocomposites based on the NBR/PVC blends. *J Appl Polym Sci*. 2019;136(25):1-11.
<https://doi.org/10.1002/app.47550>